LAWRENCE
LIVERMORE
NATIONAL
LABORATORY

LLNL-JRNL-636376

A solution to Rayleigh-Taylor instabilities: bubbles, spikes, and their scalings

K. O. Mikaelian

May 10, 2013

Physical Review E

Disclaimer

A solution to Rayleigh-Taylor instabilities: bubbles, spikes, and their scalings

Karnig O. Mikaelian
Lawrence Livermore National Laboratory, Livermore, California 94551, USA

When a fluid pushes on and accelerates a heavier fluid small perturbations at their interface grow with time and lead to turbulent mixing. The same instability, known as the Rayleigh-Taylor instability, operates when a heavy fluid is supported by a lighter fluid in a gravitational field. It has a particularly deleterious effect on initial-confinement-fusion implosions and is known to operate over 18 orders of magnitude in dimension. We propose analytic expressions for the bubble and spike amplitudes and mixing widths in the linear, nonlinear, and turbulent regimes. They cover arbitrary density ratios and accelerations that are constant or changing relatively slowly with time. We discuss their scalings and compare them with simulations and experiments.

PACS numbers 47.20.Bp, 47.20.Gv, 47.40.Nm

The Rayleigh-Taylor (RT) instability is probably the oldest and most ubiquitous phenomenon: A light fluid cannot support a heavier fluid – solids are required to support heavier objects. The opposite, however, is quite feasible: Water in a glass can support the lighter air above it, so that waves generated by swishing it will eventually die down. Turned upside down, the water spills even though it is possible, in principle, to support a perfectly flat interface in either configuration. The “heavy-over-light” configuration is

known as unstable. This is true only in a gravitational field such a g_E ($\approx 9.8\,\mathrm{m/s^2}$) which defines direction. If $g = 0$, as in outer space, either configuration is neutral meaning a small perturbation of amplitude η_0 will remain static (unless given an initial velocity $\dot{\eta}_0$).

The instability was named after Lord Rayleigh [1] and G. I. Taylor [2] who studied the linear regime. Lord Rayleigh considered only a gravitational field while Taylor added an acceleration g_P induced by pressure gradients, showing that the effective $g = g_E + g_P$. The algebraic sign is important – a glass of water in free fall is neutrally stable as in outer space: $g = 0$. While gravity is (almost) always constant in time, Taylor's extension opened the issue of man-made time-dependent $g(t)$.

The classical RT instability devoid of any stabilizing mechanism operates at all scales: nanometer-size foils driven by radiation pressure [3] to gigameter-size supernova explosions [4] and even galactic scales [5]. Of particular importance is its deleterious effect on millimeter-size inertial-confinement-fusion capsules - It is believed that the failure, so far, to achieve ignition on the National Ignition Facility may be caused by RT mixing [6]. Experiments to study this instability are carried out at scales of a few centimeters [7-14]. The purpose of this letter is to provide analytic expressions covering this vast range of scales and, with certain restrictions, a large class of $g(t)$.

As depicted in Fig. 1, there are 3 stages: Linear, nonlinear, and turbulent. The configuration and the notation is similar to experiments with liquids in a tank [7-9, 11-12,14]: A heavy fluid below the equilibrium dashed line supports a lighter fluid above, a stable configuration in $\vec{g}_E$. The tank is accelerated down with a quasi-constant g_P so that the effective $g = g_P - |g_E| \approx g_P$ with $g_P \geq 70 g_E$. A single-scale perturbation $\eta(t)\cos kx$,

$k = 2\pi/\lambda$, keeps its cosine shape during the linear regime but its amplitude $\eta(t)$ grows with time. The amplitude below the dashed line, i.e., the penetration of the lighter fluid (density ρ^l) into the heavier fluid below (density ρ^h) is denoted by η^b (b=bubble). η^s (s=spike) denotes the amplitude above the dashed line. By convention $\eta^b > 0$ and $\eta^s < 0$. In the linear regime, i.e. $\eta k << 1$, $\eta^s = -\eta^b$. In the nonlinear regime η^b still refers to the lowest penetration of ρ^l into ρ^h and conversely for η^s, but the shape is far from cosine. When the initial shape consists of several modes a turbulent mixing width develops. By convention, the 1-5% penetration depth of ρ^l into ρ^h is denoted by h^b, and conversely for h^s, *both* taken ≥ 0. We will present analytic expressions for $\eta^{b,s}$ and $h^{b,s}$ when the acceleration is constant or changing with time.

Among all relevant quantities the nonlinear spike amplitude stands out as exceptionally challenging, defying all analytic or semi-analytic descriptions. Previous models [15-16] have been found to be inadequate [16-17] when compared with exact, albeit numerical solutions, a conclusion confirmed by recent calculations [18]. We propose a new approach and a new expression for $\eta^s_{nonlinear}$, and carry over that approach to h^s to predict their behavior when $g = g(t)$.

<u>*Linear*</u>. The governing equation in the linear regime is [1,2]

$$\ddot{\eta} - gkA\eta = 0 \tag{1}$$

where $g = g(t) =$ acceleration and A is the Atwood number defined by $(\rho^h - \rho^l)/(\rho^h + \rho^l)$. When g is constant the solution is

$$\eta(t) = \eta_0 \cosh(\sqrt{gkA}t) \tag{2}$$

assuming that the initial growth rate $\dot{\eta}_0 = 0$ (otherwise a sinh term must be added.)

A closed-form solution to Eq. (1) cannot be obtained, nor should one be expected, for time-dependent accelerations. Indeed, some $g(t)$s give rise to specific instabilities known by separate names such as the Richtmyer-Meshkov instability when $g(t) = \Delta v \delta(t)$ or the Faraday instability when $g(t) = g_0 + g_1 \cos(\omega t)$.

We now obtain an analytic solution for large, slowly varying accelerations. Define

$$s(t) \equiv \int_0^t \sqrt{g(t)}dt \tag{3}$$

and use the transformation

$$\frac{d}{dt} = \sqrt{g}\,\frac{d}{ds}, \quad \frac{d^2}{dt^2} = g\,\frac{d^2}{ds^2} + \frac{\dot{g}}{2g}\frac{d}{dt} \rightarrow g\,\frac{d^2}{ds^2} \tag{4}$$

to reduce Eq. (1) to $d^2\eta / ds^2 - kA\eta = 0$ with the solution

$$\eta(t) = \eta_0 \cosh(s\sqrt{kA}). \tag{5}$$

The above transformation is useful because it requires only the calculation of $s(t)$ which is then used in Eq. (5) to find $\eta(t)$. Otherwise, Eq. (1) must be solved numerically (analytic solutions can be found for only a few $g(t)$). Even when dropping $\frac{\dot{g}}{2g}\frac{d}{dt}$ is not justified and Eq. (1) must be solved numerically Eq. (5) can serve as an estimate.

Since $\eta^s(t) = -\eta^b(t)$ both are said to "scale with s" in the linear regime. This will not be true in the nonlinear regime nor, perhaps, in the turbulent regime. We use the word "scaling" in the traditional sense, i.e., experiments or simulations with different $g(t)$s will have different $\eta(t)$s, but when plotted versus s all the curves will collapse onto one universal curve, Eq. (5).

Nonlinear. If η_0 is large or if $\eta(t)$ grows such that $\eta k \geq 1$ then the bubbles and spikes behave differently and in a more complicated way. As always, one must solve the Euler equations, a set of partial differential equations, but this must now be done numerically because they no longer simplify. We will do so using the hydrodynamic code CALE [19] and compare the numerical results with the analytic model described below.

We believe the most successful model to date has been the Layzer model [20] and its extensions [16, 21-22]. Using a "modern" notation,

$$(1+2\tilde{\eta}_2)\ddot{\eta} + k\dot{\eta}^2 + 2g\tilde{\eta}_2 = 0. \tag{6}$$

This is Layzer's Eq. (55) with the curvature function $\tilde{\eta}_2$ appropriately defined (see below), and applies for a single fluid, i.e. $A = 1$, in Cartesian coordinates, also called "2D", and for the bubble only ($\eta > 0$). For brevity and clarity we do not treat the "3D" geometry, also called "tubular flow", which parallels 2D flow with similar results [16-17, 20-21].

Applying the transformation of Eq. (4) to Eq. (6) we obtain $(1+2\tilde{\eta}_2)d^2\eta/ds^2 + k(d\eta/ds)^2 + 2\tilde{\eta}_2 = 0$. We justify below the assumption $\tilde{\eta}_2 \approx const.$ Although this equation remains a nonlinear ordinary differential equation (ODE), its solution is:

$$\eta(t) = \eta_0 + \left(\frac{1+2\tilde{\eta}_2}{k}\right)\ln[\cosh(sd\sqrt{k})] \tag{7}$$

where $d^2 \equiv -2\tilde{\eta}_2/(1+2\tilde{\eta}_2)^2$.

Layzer [20] assumed $\eta_0 = 0$ and found $\tilde{\eta}_2 \equiv \eta_2/k = -(1-e^{-3\eta k})/6$ which cannot be constant. In our extension to arbitrary η_0 we found [21]

$$\tilde{\eta}_2 \equiv \eta_2 / k = -\{1 + (3\eta_0 k - 1)e^{-3k(\eta-\eta_0)}\}/6 . \quad (8)$$

It follows that if $\eta_0 = \eta^* \equiv 1/3k$ then $\tilde{\eta}_2$ can be constant, equal to -1/6, giving $d = \sqrt{3}/2$.

Layzer's model for bubbles was generalized to arbitrary A by Goncharov [16]: Eq. (6) is replaced by a substantially more complicated but still a second-order ODE. Eq. (8), however, remains the same and therefore the solution to Goncharov's ODE can be obtained by a rather simple transformation for $\tilde{\eta}_2 = const. = -1/6$. Applying Eq. (4) to that solution we obtained [23]

$$\eta^b(A) = \eta_0 + \left(\frac{3+A}{3(1+A)k}\right)\ln[\cosh(s\sqrt{6kA(1+A)}/(3+A))] . \quad (9)$$

This is the bubble amplitude for arbitrary A. Of course $s = \sqrt{g}t$ for constant g.

The spike is much more challenging. For $A = 1$ Zhang proposed [22] using Layzer's equation, Eq. (6), with a negative η and a positive η_2 just as one does in the linear regime (η and η_2 always have opposite signs). The curvature η_2 can no longer be taken to be constant but instead approaches $+\infty$ – See Eq. (8) with η large and negative. We pointed out [23] that this requires $\eta^s(1)$ to scale with Δx defined by

$$\Delta x \equiv \int[\int g(t)dt]dt . \quad (10)$$

The argument is as follows: For very large η_2 Eq. (6) requires that $\ddot{\eta} + g = 0$ hence $\eta \sim -\Delta x$. Here we propose

$$-\eta^s(1) = \eta_0 + \frac{1}{k}\ln[\cosh(k\Delta x)] . \quad (11)$$

Of course $\Delta x = gt^2/2$ for constant g. This expression is in fair agreement with solutions to Eq. (6) with a negative η, particularly for large $|\eta_0|$, as proposed by Zhang [22] for a constant acceleration.

The last and no doubt most important element is $\eta^s(A)$, the nonlinear spike amplitude for arbitrary A. Numerical simulations [18, 24-25] reveal a complex structure exacerbated by coupling to secondary instabilities such as the KH (Kelvin-Helmholtz) instability. This coupling was absent in the single-fluid case allowing potential-flow-models like Layzer's to provide an adequate description of $\eta^s(1)$ either as an ODE like Eq. (6) or explicitly like Eq. (11). When a second fluid is present the KH instability makes such an approach intractable.

Instead, we propose a different approach: Interpolation. We know that $\eta^s(A)$ is anchored at the two extreme ends of A: For $A \approx 0$ or $A << 1$, $\eta^s(A) \approx -\eta^b(A)$ given by Eq. (9). For $A = 1$, $\eta^s(1)$ is given, at least approximately, by Eq. (11). All we need is to interpolate between these two ends, guided by numerical simulations. We propose

$$-\eta^s(A) = \eta^b(A)\left\{1 + \left[0.4 + 0.6A^{10}\right]\left[\left(\frac{-\eta^s(1)}{\eta^b(A)}\right)^A - 1\right]\right\}. \qquad (12)$$

We carried out several CALE simulations of Linear Electric Motor [11-12] or LEM-like experiments of which we show two in Fig. 2, $A = 0.48$ and $A = 0.81$. The 7.3 cm-wide tank accelerates down at a constant $100 g_E = 0.098\,\text{cm/ms}^2$ and has 3 initially sinusoidal perturbations with $\eta_0 = 0.13\,\text{cm}$. The insets show the interfaces between the two fluids at 20 ms. Notice the complexity of the spikes compared with the relative

simplicity of the bubbles. The dashed lines are from CALE, the continuous lines from Eq. (9) for the bubbles and Eq. (12) for the spikes.

Perhaps the most important deduction from the above discussion is that $\eta^s(A)$, given by Eq. (12), *scales neither with* s *nor with* Δx, *but is a mixture of both*. In other words, the traditional approach of varying $g(t)$ and plotting $\eta^s(A)$ as a function of either $s(t)$ or $\Delta x(t)$ will *not* collapse to a single curve. It *will* collapse to the s–curve for $A<<1$ where $\eta^s(A) \approx -\eta^b(A)$, and to the Δx–curve for $A=1$, but for intermediate values of A neither scaling is valid.

We ran a number of CALE simulations to verify the above observation. An example is shown in Fig. 3: The same LEM-tank is subjected to a quadratically increasing $g(t) \sim t^2$ reaching $1000 g_E$ in 15 ms. The CALE curves, again in dashes, are compared with the analytic expressions: Eq. (9) for the bubbles and Eq. (12) for the spikes. Fig. 3 shows that this approach is in good agreement with direct numerical simulations. We obtained equally good (and sometimes better) agreement with other acceleration histories such as $g(t) \sim t^n$, $n=1-5$, or $g(t) \sim te^{-t^2}$.

<u>*Turbulent*</u>. Random perturbations, initially very small, are observed experimentally to grow into turbulent mixing layers $h^{b,s}$ evolving with time [8, 10-14]. This regime is both more diffcult and yet, in some sense, "easier" than the previous one. It is difficult because there is no equation corresponding to Eq. (1) or Eq. (6) whose solution gives $h^{b,s}$. It requires extremely large 3-dimensional hydrocode simulations [26] (beyond our present capability) for a numerical solution. On the other hand, experiments [8, 10-14] have indicated a relatively simple behavior when g is constant:

$$h^{b,s} = \alpha^{b,s} A g t^2 . \tag{13}$$

The absence of any single-scale k, plus the limit $h^{b,s}(t=0) \approx 0$ lead directly to the form given above: gt^2 is the only length scale available if g is constant. If g varies with time then it must involve at least one time-constant, call it T, and then $h = f(A, gt^2, t/T)$ cannot be determined by any dimensional argument.

Experiments indicate that α^b is a constant between 0.03 [14] and 0.07 [8, 10-13] independent of A, while α^s depends on A: At low A $\alpha^s \approx \alpha^b$, and increases with A to become 4-5 times α^b [12]. Since this behavior is similar to $|\eta^s(A)|$, we compared the experimental results with an expression very similar to Eq. (12):

$$\alpha^s(A) = \alpha^b \left\{1 + (0.4 + 0.6A^{10})(r^A - 1)\right\} \tag{14}$$

where $r = \alpha^s(1)/\alpha^b \approx 4.5$, taking $\alpha^b \approx 0.05$ from the same work [12]. Eq. (14) is shown in Fig. 4 and it compares well with the data recorded for constant g.

Eq. (14) follows from

$$h^s(A) = h^b(A)\left\{1 + \left[0.4 + 0.6A^{10}\right]\left[\left(\frac{Ah^s(1)}{h^b(A)}\right)^A - 1\right]\right\}, \tag{15}$$

recovering Eq. (14) for constant g: $Ah^s(1)/h^b(A) = A\alpha^s(1)gt^2/\alpha^b Agt^2 = \alpha^s(1)/\alpha^b$. Of course $h^s(A) \approx h^b(A)$ for low A and $h^s(A \to 1) = h^s(1)$.

We now turn to scaling. Experimentally, Read [8] showed that h^b scales with s, i.e.,

$$h^b(A) = \alpha^b A s^2, \tag{16}$$

also confirmed by LEM experiments [11]. As far as we know, there has been only one study, again experimental, of h^s scaling, indicating that $h^{b,s}$ *both* scale with s [12]. We

call this "conventional scaling". However, this was done at a low Atwood number $A = 0.22$ where one expects $h^s \approx h^b$. Here we conjecture another possibility: $h^s(1)$ scales with Δx, i.e.,

$$h^s(1) = 2\alpha^s(1)\Delta x, \tag{17}$$

and Eq. (15) is valid, as is, with $h^b(A)$ given by Eq. (16) and $h^s(1)$ by Eq. (17). Note that $r \equiv Ah^s(1)/h^b(A) = 2A\alpha^s(1)\Delta x/\alpha^b As^2 = 2(\alpha^s(1)/\alpha^b)\Delta x/s^2 \approx 9\Delta x/s^2$. We recover Eq. (14) for constant g: $\Delta x = s^2/2$, $r \approx 4.5$.

Conventional scaling predicts $h^s(A)/h^b(A) = \alpha^s(A)/\alpha^b = 1 + (0.4 + 0.6A^{10})(r^A - 1)$ with $r \approx 4.5$ for *any* $g(t)$ *and for all* t. In contrast, our scaling predicts $r \approx 9\Delta x/s^2$ whose value depends on $g(t)$ and, except for one case, on t. Let us start with the exception: When $g(t) \sim t^n$, $\Delta x/s^2 = (n+2)/4(n+1)$. The ratio h^s/h^b will again be time-independent for this $g(t)$, but its value will still differ from conventional. For example, take $n = 2$: $\Delta x/s^2 = 1/3$ hence $r \approx 3$, compared with the conventional $r \approx 4.5$. The ratio h^s/h^b will be 1.3 and 1.7, compared with the conventional 1.4 and 2.1, for $A = 0.48$ and $A = 0.81$ respectively. Since both scalings give $h^s \approx h^b$ at low A one must obviously look at large A to discern the difference.

Any other $g(t)$ will result in a time-dependent h^s/h^b in our model. We show an example with $A = 0.81$ in the inset of Fig. 4 for the case $g(t) \sim te^{-t^2}$ reaching a maximum of $170g_E$ at ~7 ms. The inset shows $g(t)$ in units of $100g_E$ and h^b, which is the same (Eq. (16)) in both models. In red we show h^s according to the two different scalings: Conventional ($r = 4.5$) and the new proposal ($r = 9\Delta x/s^2$). Between $t = 0$ and

$t = 30\,\text{ms}$ h^s / h^b varies from 1.8 to 3.3 in our scaling, while it is always a constant (≈ 2.1 for $A = 0.81$) with conventional scaling. At 30 ms our spike is $3.3/2.1 \approx 1.6$ times larger than conventional.

In conclusion, we propose that all bubble amplitudes $\eta^b(A)$ or mixing widths $h^b(A)$ scale with s as in Eqs. (5), (9), and (16). The *linear* spike amplitude also scales with s because $\eta^s_{linear} = -\eta^b_{linear}$. The *nonlinear* $\eta^s(1)$ scales with Δx – Eq. (11). The nonlinear $\eta^s(A)$ has a mixed scaling – Eq. (12). The turbulent $h^s(1)$ scales with Δx – Eq. (17). And, finally, $h^s(A)$ has a mixed scaling – Eq. (15).

We thank Guy Dimonte for supplying the experimental data on α^b and α^s. This work was performed under the auspices of the U. S. Department of Energy by Lawrence Livermore National Laboratory under Contract DE-AC52-07NA27344.

REFERENCES

[1] Lord Rayleigh, *Scientific Papers*, **2**, (Cambridge, England, 1900).

[2] G. I. Taylor, Proc. R. Soc. London Ser. A **201**, 192 (1950).

[3] C. A. J. Palmer et al., Phys. Rev. Lett. **108**, 225002 (2012).

[4] C. C. Joggerst, A. Almgren, and S. E. Woosley, Ap. J. **723**, 353 (2010).

[5] G. S. Novak, J. P. Ostriker, and L. Ciotti, Ap. J. **737**, 26 (2011).

[6] S. P. Regan *et al*., Phys. Plasmas **19**, 056307 (2012).

[7] R. Popil and F. L. Curzon, Rev. Sci. Instrum. **50**, 1291 (1979).

[8] K. I. Read, Physica D **12**, 45 (1984).

[9] J. W. Jacobs and I. Catton, J. Fl. Mech. **187**, 353 (1988).

[10] D. M. Snider and M. J. Andrews, Phys. Fl. **6**, 3324 (1994).

[11] G. Dimonte and M. Schneider, Phys. Rev. E **54**, 3740 (1996).

[12] G. Dimonte and M. Schneider, Phys. Fluids **12**, 304 (2000).

[13] P. Ramaprabhu and M. J. Andrews, J. Fl. Mech. **502**, 233 (2004).

[14] D. H. Olson and J. W. Jacobs, Phys. Fl. **21**, 034103 (2009).

[15] U. Alon *et al*., Phys. Rev. Lett. **74**, 534 (1995).

[16] V. N. Goncharov, Phys. Rev. Lett. **88**, 134502 (2002).

[17] K. O. Mikaelian, Phys. Rev. E **78**, 015303 (2008).

[18] P. Ramaprabhu *et al*., Phys. Fl. **24**, 074107 (2012).

[19] R. E. Tipton, CALE Users Manual (unpublished) and in *Megagauss Technology and Pulsed Power Applications*, edited by C. M. Fowler, R. S. Caird, and D. J. Erickson (Plenum, New York, 1987), p. 299.

[20] D. Layzer, Astrophys. J. **122**, 1 (1955).

[21] K. O. Mikaelian, Phys. Rev. Lett. **80**, 508 (1998).

[22] Q. Zhang, Phys. Rev. Lett. **81**, 3391 (1998).

[23] K. O. Mikaelian, Phys. Rev. E **81**, 016325 (2010).

[24] G. R. Baker, D. I. Meiron, and S. A. Orszag, Phys. Fl. **23**, 1485 (1980).

[25] G. Tryggvason, J. Comp. Phys. **75**, 253 (1988).

[26] G. Dimonte *et al*. (ALPHA-Group), Phys. Fl. **16**, 1668 (2004).

Figure Captions

Fig. 1. Schematic drawing of the RT instability in the linear, nonlinear, and turbulent regimes.

Fig. 2. (Color online) Bubble and spike amplitudes as functions of time for a $g = const. = 100 g_E$ problem with two different Atwood numbers: $A = 0.48$ (red) and $A = 0.81$ (black). By convention $\eta^b > 0$ and $\eta^s < 0$. The LEM-like tank is 7.3 cm wide and starts with 3 sinusoidal perturbations of amplitude $\eta_0 = 0.13\,\text{cm}$. The dashed lines show $\eta^{b,s}$ as calculated by CALE. The analytic, continuous curves are calculated using Eq. (9) for η^b and Eq. (12) for η^s. Snapshots at 20 ms.

Fig. 3. (Color online) Same as Fig. 2 for a quadratically increasing acceleration $g(t) = 1000 g_E (t/15)^2$, t in ms. Snapshots at 15 ms.

Fig. 4. (Color online) α^b and α^s as functions of Atwood number A. We take $\alpha^b = 0.05$ (black) and Eq. (14) for $\alpha^s(A)$ (red). Experimental data from Ref. [12]. The inset shows $h^{b,s}$ as functions of time for $g(t) \sim te^{-t^2}$ shown as a dashed curve in units of

$100 g_E$. We have used Eq. (16) for h^b (black) and Eq. (15) for h^s (red) with $r \equiv Ah^s(1)/h^b(A) = \alpha^s(1)/\alpha^b \approx 4.5$ for conventional scaling, and $r = 2\alpha^s(1)\Delta x/\alpha^b s^2 \approx 9\Delta x/s^2$ for the new proposed scaling. At 30 ms the new scaling predicts a spike 1.6 times larger than conventional – see text.

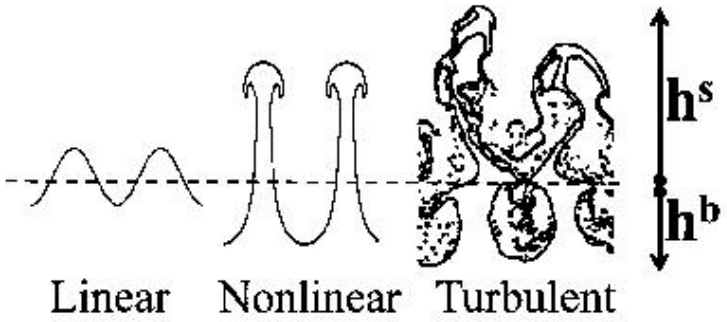

Fig. 1

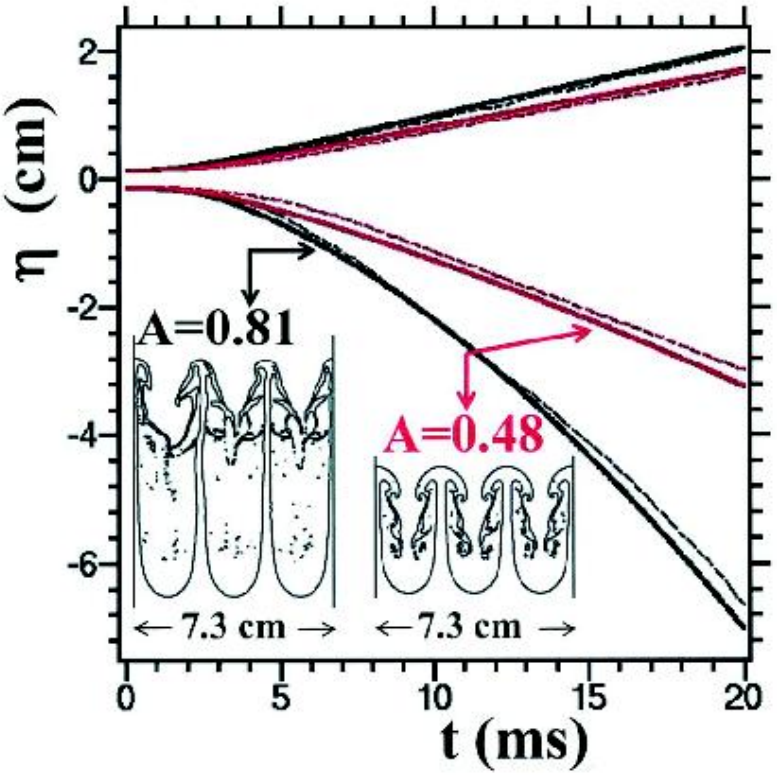

Fig. 2

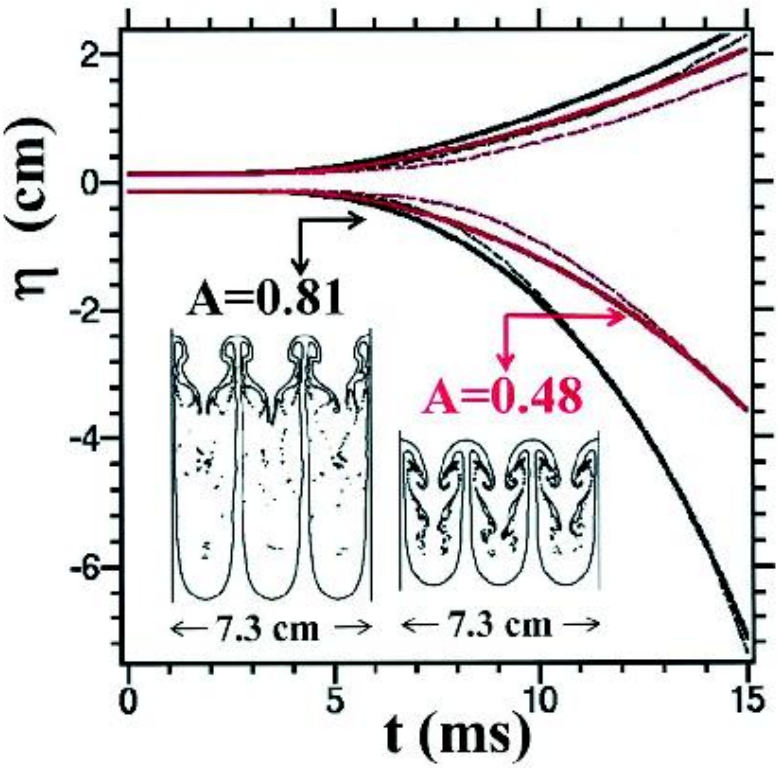

Fig. 3

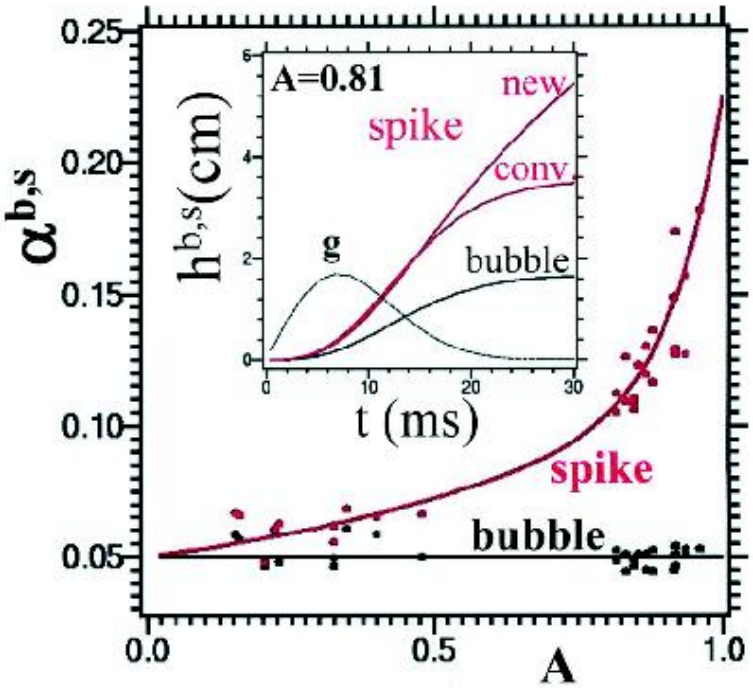
0.25
0.20
0.15
0.10
0.05
$\alpha^{b,s}$
0.0
0.5
1.0
A
spike
bubble
A=0.81
new
spike
conv
g
bubble
$h^{b,s}$(cm)
t (ms)
0
10
20
30
2
4
6

Fig. 4